

Ordered Macroporous Particles by Colloidal Templating

Gi-Ra Yi, Jun Hyuk Moon, and Seung-Man Yang*

Department of Chemical Engineering, Korea Advanced Institute of Science and Technology,
373-1 Kusong-dong, Yusong-ku, Taejeon 305-701, Korea

Received March 22, 2001. Revised Manuscript Received May 24, 2001

Ordered macroporous particles of silica and titania were fabricated by colloidal templating. The colloidal templates were assembled through colloidal crystallization of suspended polystyrene latex sphere particles in aqueous droplets straddling an air–oil interface. The procedures involve first preparing spherical colloidal crystalline particles of polystyrene latex spheres and then infusing them with metal precursor solutions that form silica or titania in the interstices. Finally, calcination decomposes the polystyrene latex spheres, leaving macropores at their sites. The shape of the template was controlled by the presence of additive surfactant or by the action of an applied electric field. Specifically, spherical, concave disklike, and ellipsoidal colloidal crystals were prepared successfully and used as templates for the fabrication of ordered macroporous particles. The SEM images of the prepared macroporous particles showed that the pores were interconnected and ordered into a hexagonal arrangement.

Introduction

Ordered macroporous materials have received much attention in the past decade due to their potential application in various areas of separation processes, catalysis, photonic band gap (PBG) materials, and other emerging nanotechnologies.¹ Colloidal templating is one of the controllable and widely applicable methods to fabricate such structural materials.^{2,3} Since ordered macroporous silica was produced in 1997, a variety of macroporous ceramics, metals, semiconductors, and polymers with well-defined pore sizes in the sub-micrometer range have been successfully synthesized by use of the self-assembled templates of colloidal spheres.⁴ Typical building blocks of the self-assembly are polystyrene (PS) or poly(methyl methacrylate) (PMMA) latex spheres, silica spheres, and emulsion droplets with narrow size distribution.^{4–16} However, the macroscopic structures of macroporous materials in the prior studies have been in the form of irregular shapes.

For practical applications, the macroporous materials should be shaped into usable objects on a large length scale. Such shaped macroporous materials could be produced from the colloidal crystals with desired shape.

A number of methods for shaped colloidal crystals have been exploited using colloidal crystallization, including flow of the colloids through micromachined channels or a smooth narrow pore membrane, and proper use of capillary forces.^{8,17–19} One of the simplest approaches was developed by Velev et al. to use “*suspension droplet*” as a confined geometry (i.e., a liquid droplet containing a number of colloidal particles inside). This method can lead to highly ordered colloidal assemblies through the crystallization of submicron-sized colloidal particles during evaporation of water in the suspension droplets straddling the air–oil interface.^{20,21} Recently, we have extended Velev’s method to the fabrication of nonspherical colloidal assemblies by application of an electric field.²²

Here we first report on the preparation of ordered macroporous particles from colloidal assemblies that were regular in shape, such as spheres, ellipsoids, and concave disks. Specifically, the procedures contained three steps. First, the colloidal assemblies were fabricated by the colloidal crystallization of suspension droplets following the procedure reported in the literature.²⁰ The building blocks of the colloidal crystal were monodisperse polystyrene (PS) latex spheres. The shape of colloidal assemblies that were used as templates was controlled by adding surfactant or by applying an ac electric field.^{20,22} Second, the colloidal crystals were

* To whom correspondence should be addressed. E-mail: smyang@kaist.ac.kr.

(1) Velev, O. D.; Lenhoff, A. M. *Curr. Opin. Colloid Interface Sci.* **2000**, *5*, 56.

(2) Xia, Y. N.; Gates, B.; Yin, Y. D.; Lu, Y. *Adv. Mater.* **2000**, *12*, 693.

(3) Velev, O. D.; Kaler, E. W. *Adv. Mater.* **2000**, *12*, 531.

(4) Velev, O. D.; Jede, T. A.; Lobo, R. F.; Lenhoff, A. M. *Nature* **1997**, *389*, 447.

(5) Imhof, A.; Pine, D. *Nature* **1997**, *389*, 948.

(6) Holland, B. T.; Banford, C. F.; Stein, A. *Science* **1998**, *281*, 538.

(7) Zakhidov, A. A.; Baughman, R. H.; Iqbal, Z.; Cui, C.; Khayrullin, I.; Dantas, S. O.; Marti, J.; Ralchenko, V. G. *Science* **1998**, *282*, 897.

(8) Subramanian, G.; Manoharan, V. N.; Thorne, J. D.; Pine, D. J. *Adv. Mater.* **1999**, *11*, 1261.

(9) Wijnhoven, J. E. G. J.; Vos, W. L. *Science* **1998**, *281*, 802.

(10) Vlasov, Y. A.; Yao, N.; Norris, D. J. *Adv. Mater.* **1999**, *11*, 165.

(11) Braun, P. V.; Wiltzius, P. *Nature* **1999**, *402*, 603.

(12) Yi, G.-R.; Yang, S.-M. *Chem. Mater.* **1999**, *11*, 2322.

(13) Jiang, P.; Cizeron, J.; Bertone, J. F.; Colvin, V. L. *J. Am. Chem. Soc.* **1999**, *121*, 7957.

(14) Yan, H.; Banford, C. F.; Holland, B. T.; Parent, M.; Smyrl, W. H.; Stein, A. *Adv. Mater.* **1999**, *11*, 1003.

(15) Velev, O. D.; Tesser, P. M.; Lenhoff, A. M.; Kaler, E. W. *Nature* **1999**, *401*, 548.

(16) Jiang, P.; Bertone, J. F.; Colvin, V. L. *Science* **2001**, *291*, 453.

(17) Gates, B.; Yin, Y.; Xia, Y. *Chem. Mater.* **1999**, *11*, 2827.

(18) Velev, O. D.; Jede, T. A.; Lobo, R. F.; Lenhoff, A. M. *Chem. Mater.* **1998**, *10*, 3597.

(19) Jiang, P.; Bertone, J.; Hwang, K.; Colvin, V. *Chem. Mater.* **1999**, *11*, 2132.

(20) Velev, O. D.; Lenhoff, A. M.; Kaler, E. W. *Science* **2000**, *287*, 2240.

(21) Velev, O. D.; Furusawa, K.; Nagayama, K. *Langmuir* **1996**, *12*, 2373.

(22) Yi, G.-R.; Moon, J. H.; Yang, S.-M. *Adv. Mater.*, in press.

Table 1. Preparation Recipe and Characteristics of the Polystyrene Beads Used in the Present Study

sample	NaSS (M)	diameter (nm)/polydispersity (DLS)	diameter (nm) (SEM)	ζ (mV)	PH
B	0.30	199/0.005	190	-43.1	4.18
C	0.15	235/0.005	230	-39.3	4.27
D	0.10	293/0.005	275	-37.5	4.20

infused with metal oxide precursor solutions that were converted into silica or titania in the interstices between the PS spheres. Third and finally, the PS latex spheres were removed by calcination, which left macropores at their sites. The structured particles of various regular shapes were in the range of a few millimeters in size and possessed ordered macropores a few hundred nanometers in diameter. Since the prepared microstructured materials have two distinctively different length scales, they are of practical significance in wide areas of applications such as photocatalysts, size-exclusive chromatography, electrodes of solar cell, and photonic crystals.^{23–28}

Experimental Section

Synthesis of Uniform Latex Particles. Non-cross-linked, monodisperse PS latex particles were synthesized by emulsifier-free emulsion polymerization²⁹ using potassium persulfate as initiator and potassium bicarbonate as buffer. In the present study, the PS latex spheres with three different diameters were synthesized by varying the concentration of a comonomer, sodium styrene sulfonate (NaSS, Sigma), keeping all other experimental conditions unchanged. Table 1 contains the NaSS concentrations and characteristics for the PS beads prepared in the present study. As noted, NaSS could control the diameter and surface charge (or ζ potential) of the PS latex spheres. Typical scanning electron microscopy (SEM) images of the prepared PS latex spheres of 275, 230, and 190 nm diameter were reproduced in parts A, B, and C of Figure 1, respectively. Particle size was estimated by both the SEM images and photon correlation spectroscopy (Brookhaven with BI200SM goniometer), which also determined its polydispersity. The ζ potentials of the prepared latices were measured from the electrophoretic mobility by ZetaPlus (Brookhaven).

Colloidal Crystallization of Suspension Droplets at an Air–Oil Interface. Figure 2 is a schematic of the crystallization cell. We could apply an electric field to the droplet-template colloidal crystallization cell with electrodes that were connected to an alternating current (ac) electric power supply. The suspension droplet of the monodisperse PS latex spheres was straddling the air–oil interface, but with most of the suspension droplet immersed in the oil phase. If necessary, an ac electric field was applied to deform the suspension droplets. During evaporation of the drop-phase liquid (i.e., water in the present case), the PS latex spheres in the suspension droplets began to order into a macrocrystalline structure. In the presence of an applied electric field, the suspension droplets deformed into spheroids. The suspension droplets, of initial volume 10–40 μL , contained 10–50% in volume of negatively charged PS latex microspheres 190–275 nm in diameter. We used viscous silicone oil (Shin-Etsu: KF-54, $\mu = 0.4 \text{ Pa}\cdot\text{s}$) or partially fluorine-substituted silicone oil (Shin-Etsu: FL100-1000cs, $\mu = 1.0 \text{ Pa}\cdot\text{s}$) as the continuous oil phase

(23) Zhao, D.; Sun, J.; Li, Q.; Stucky, G. D. *Chem. Mater.* **2000**, *12*, 275.

(24) Lin, H.-P.; Cheng, Y.-R.; Mou, C.-Y. *Chem. Mater.* **1998**, *10*, 3772.

(25) Stone, V. F.; Davis, R. J. *Chem. Mater.* **1998**, *10*, 1468.

(26) Caruso, R. A.; Giersig, M.; Willig, F.; Antonietti, M. *Langmuir* **1998**, *14*, 6333.

(27) Barbe, C. J.; Arendse, F.; Comte, P.; Jirousek, M.; Lenzmann, F.; Shklover, V.; Grätzel, M. *J. Am. Ceram. Soc.* **1997**, *80*, 3157.

(28) Schacht, S.; Huo, Q.; Voigt-Martin, I. G.; Stucky, G. D.; Schüth, F. *Science* **1996**, *273*, 768.

(29) Kim, J. H.; Chainey, M.; El-Aasser, M. S.; Vanderhoff, J. W. *J. Polym. Sci. A: Polym. Chem.* **1989**, *27*, 3187.

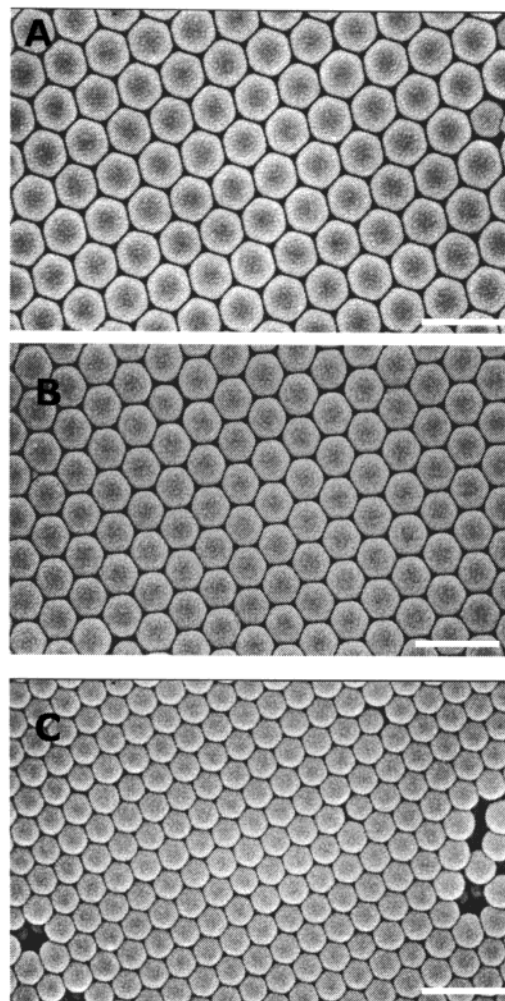


Figure 1. Typical SEM images of polystyrene latex spheres with diameters 275 nm (A), 230 nm (B), and 190 nm (C), respectively. Scale bars are 500 nm.

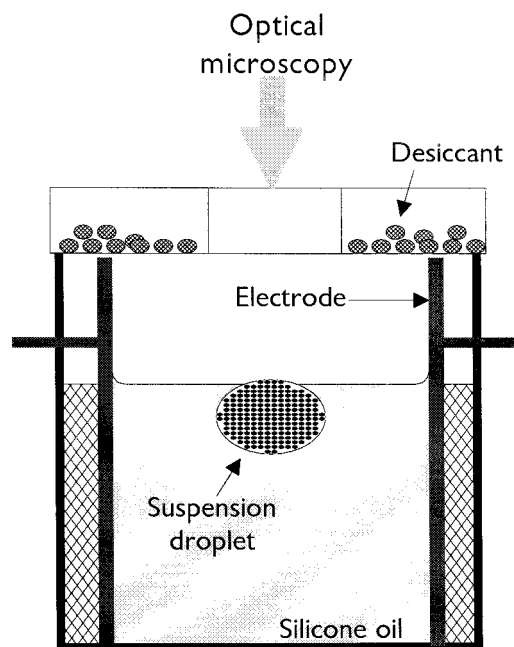


Figure 2. Schematic of the colloidal crystallization cell with a suspension droplet as template.

for electric-field-induced deformation, and otherwise, we used perfluoromethyldecalin (Aldrich) as the continuous oil phase.

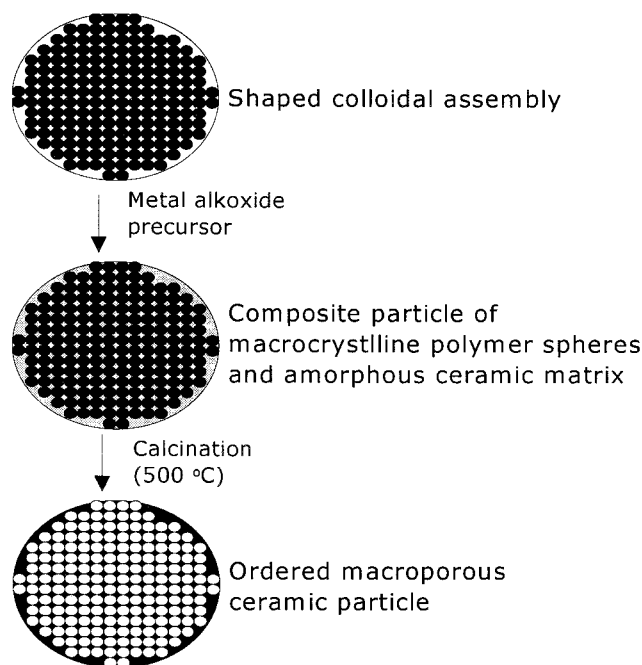


Figure 3. Schematic diagram of the colloidal templating method for the fabrication of ordered macroporous particles. The supraparticle formed by PS latex spheres was used as template.

The suspension droplets underwent shrinkage during incubation for about 12 h, which depended on initial particle volume fraction. Finally, the oil that was infiltrated into the macrocrystalline structure was extracted with hexane and dried to produce supraparticle assemblies of various shapes.

Synthesis of Ordered Macroporous Particles. Figure 3 illustrates the synthetic procedure of ordered macroporous particles. Macrocrystalline colloidal assemblies with spherical, concave disklike, and ellipsoidal shapes, which were produced in the droplet-template colloidal crystallization cell, were infused within a metal alkoxide precursor solution such as titanium(IV) tetraisopropoxide (TTIP: 97% $\text{Ti}(\text{OCH}(\text{CH}_3)_2)_4$, Aldrich) and tetramethyl orthosilicate (TMOS: 98% $\text{Si}(\text{OCH}_3)_4$, Aldrich). This process was conducted under moisture-free conditions because of its high reactivity with water. After about 2 h, macrocrystalline spheres containing the infiltrated precursor solution were pulled out. Then, composite particles of macrocrystalline PS latex spheres and an amorphous ceramic matrix were synthesized through sol-gel reaction. TTIP and TMOS used as titania and silica precursors, respectively, were hydrolyzed with moisture from the atmosphere. Finally, PS latex spheres constituting the composite colloidal crystals were removed by calcination at 500 °C for 5 h. The heating rate was fixed at 1 °C/min. The internal pore structure was observed through the SEM images taken with a LEO 1400 scanning electron microscope at 20 kV.

Results and Discussion

Spherical Ordered Macroporous Particles. Spherical colloidal crystals that were assembled in the droplet-template colloidal crystallization cell were used as templates for spherical macroporous materials. The PS spheres in the aqueous suspension droplets that were placed on the surface of perfluoromethyldecalin were concentrated by evaporating the water. The change of droplet size during evaporation was plotted as a function of the incubation time in Figure 4A. Indeed, the size decreased monotonically with time. As the PS sphere concentration exceeded a certain transition value, the PS latex spheres began to order into a face-centered cubic (fcc) structure. The spherical supraparticle as-

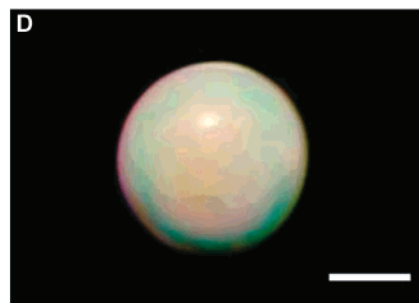
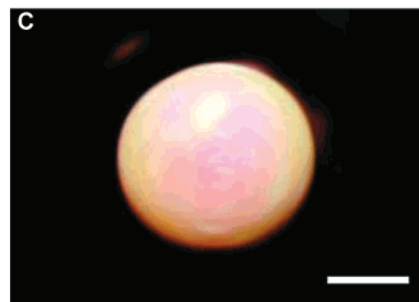
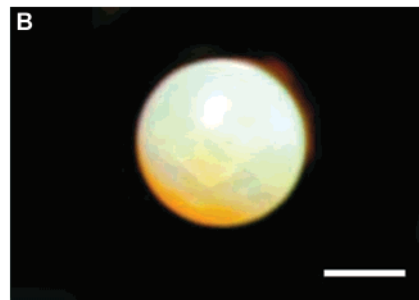
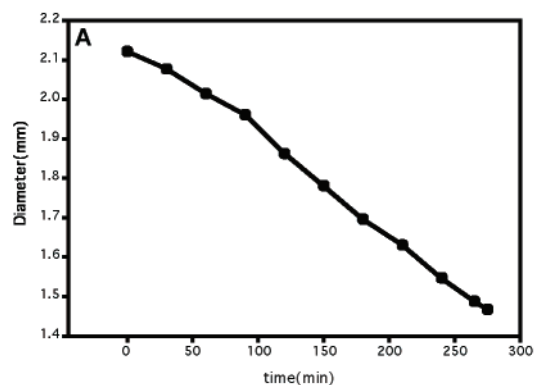


Figure 4. (A) Diameter of a suspension droplet as a function of the incubation time during the colloidal crystallization. The suspension droplet contained the PS latex spheres of 230 nm diameter. (B–D) Optical micrographs of the structured spherical assemblies formed by the PS latex spheres of three different diameters, 190, 230, and 275 nm, respectively. In each case, the scale bar is 1 mm.

semblies reflected various colors depending on the PS sphere diameter, as shown in Figure 4B–D. The colors arise from light diffraction (opalescence) from the colloidal arrays. This is clear evidence of long-range ordering of the latex spheres as shown in the SEM image of Figure 5 for the internal arrangement of a colloidal crystal of PS latex spheres.

The prepared macrocrystalline particles were soaked in a solution of metal alkoxide precursor, which went

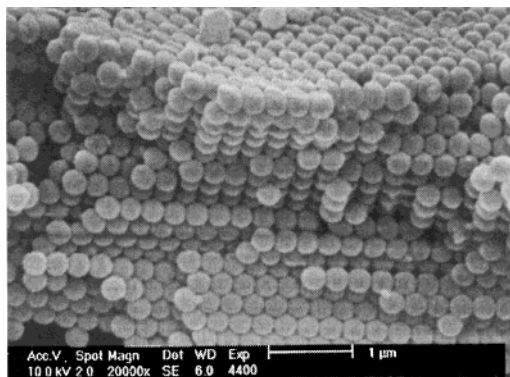


Figure 5. Typical SEM image of a structured spherical assembly formed from the PS latex spheres 230 nm in diameter.

through the interstices between the PS latex spheres by capillary force. Then the macrocrystalline spheres into which the precursor fully infiltrated were pulled out and exposed to the air. With moisture in the air, the metal oxide precursor was hydrolyzed. It is especially noteworthy that before the hydrolysis reaction proceeded, the residual alkoxide precursor remaining on the surface of spherical colloidal assemblies should be removed. Otherwise, a thick skin was formed on the ordered macroporous sphere. In this study, the skin formation was avoided by removing precursor solution on the surface of colloidal assemblies in a moisture-free space or by treating with *n*-propanol. Finally, the polystyrene latex spheres constituting the organic–inorganic composite microstructured particles were removed by calcination at 500 °C for 5 h, leaving ordered spherical air voids at their sites in the matrix of titanium oxide (Figure 6) or silicon oxide (Figure 7). The size of the air voids ranged from 120 to 200 nm. All samples underwent shrinkage during calcination. Nevertheless, spherical shapes of colloidal crystals were kept, as shown from a low-magnification image of an optical microscope (see parts A of Figures 6 and 7). The SEM images reproduced in parts B of Figures 6 and 7 showed that calcined samples of titanium and silicon oxides were highly ordered in three-dimensions over the entire range, resembling a cubic close packing of cages. As noted from the SEM images, the ordered pore arrangement is partially obscured by the roughness of the fracture surface. However, the cubic close packing structure is clearly seen from the two-dimensional Fourier transforms (FFTs) of the corresponding SEM images (see insets B of Figures 6 and 7). The resulting spot pattern indicates that the image plane is close to the (111) plane of the fcc lattice. The void spaces were interconnected in three dimensions through windows whose diameters typically exceeded 40 nm, and wall thickness was about 40 nm for titanium oxide (TiO₂) and 50 nm for silicon oxide (SiO₂); see parts C of Figures 6 and 7. The thermal gravimetric analysis in Figure 8 shows that the organic PS particles were completely decomposed at high temperatures between 400 and 450 °C for both TiO₂ and SiO₂. The crystal phase of titanium oxide was identified by powder X-ray diffraction (PXRD) of the bulk sample. As shown in Figure 9, the sample displayed a typical anatase peak, which is of practical significance as a potential application to photocatalyst.³⁰ In addition, we performed a BET experiment to inves-

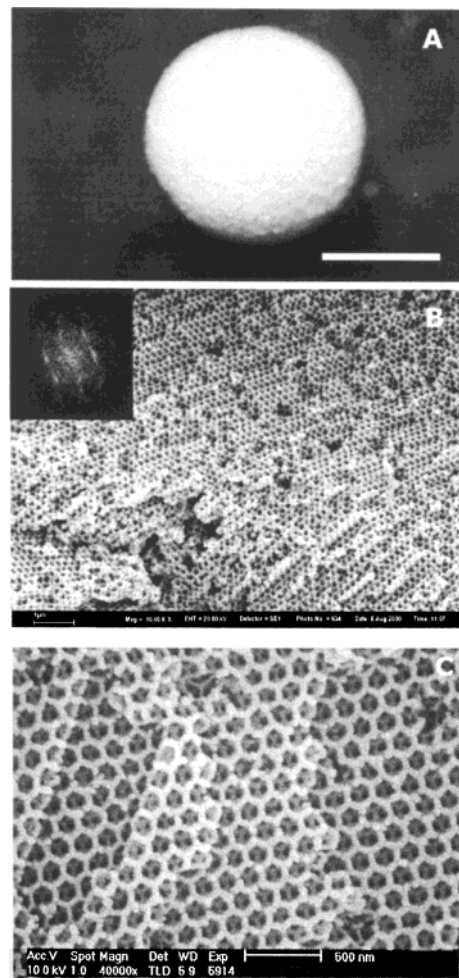


Figure 6. (A) Optical microscope image of an ordered macroporous titania sphere that was synthesized by templating of the spherical colloidal assembly formed from the 230 nm PS spheres. The scale bar denotes 1 mm in length. (B) Typical SEM image of an ordered macroporous titania sphere. The inset shows the fast Fourier transform of the SEM image. (C) SEM image at large magnification showing the interconnected cavity pores.

tigate the microporosity inside the prepared macroporous materials. For titania, the BET surface area was 58.8 m²/g and the average pore diameter was 12.2 nm, and for silica, the BET surface area was 187.8 m²/g and the average pore diameter was 9.7 nm.

Nonspherical Ordered Macroporous Particles.

The shape of the macroporous particle prepared from the present colloidal templating is determined by the shape of the suspension droplet. There are a few ways to control the shape of the suspension droplet.²⁰ In this work, the nonspherical suspension droplets were formed either by adding a surfactant or by applying an external electric field.^{20,22} The nonspherical suspension droplets led to the formation of concaved disklike or ellipsoidal colloidal assemblies and ordered macroporous particles.

Concaved Disklike Shape. When surfactant is added to the aqueous suspension drop phase, the tensions of the two (air–water and water–oil) interfaces are reduced. As the surfactant concentration increases, the interfacial tension between silicon oil and air becomes

(30) Mills, A.; Le Hunte, S. *J. Photochem. Photobiol. A: Chem.* **1997**, *108*, 1.

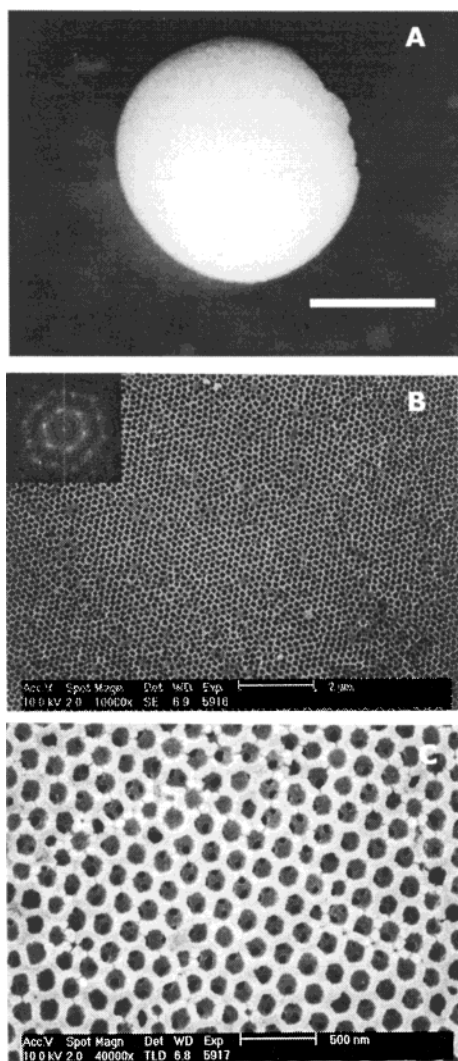


Figure 7. (A) Optical microscope image of an ordered macroporous silica sphere that was synthesized by templating of the spherical colloidal assembly formed from the 230 nm PS spheres. The scale bar denotes 1 mm in length. (B) Typical SEM image of an ordered macroporous silica sphere. The inset shows the fast Fourier transform of the SEM image. (C) SEM image at large magnification showing the interconnected cavity pores.

predominant. Under these circumstances, the suspension droplet straddling the oil–air interface is pulled out and forms a lens-shaped globule. Furthermore, when the air–oil interfacial tension is too strong for the tensions of the two (air–water and water–oil) interfaces, the suspension droplet flattens into a concave disk. Velev et al. prepared well-structured doughnut-like colloidal assemblies by adding sodium perfluorooctanoate as a surfactant into the aqueous phase.²⁰ In the present work, we also prepared concaved disklike colloidal assemblies as shown in Figure 10A by adding ethoxylated nonionic fluorosurfactant (Zonyl FSN, Dupont) into the aqueous phase. The droplet shape tends to flatten into a concaved disklike shape as the surfactant concentration increases up to 15 wt %. Following the same procedure that we used in the preparation of spherical macroporous particles, *concaved disklike* macroporous titania particles were synthesized by using the disklike colloidal assemblies as templates. The microscope image of the prepared concaved disklike macroporous particle is shown in Figure 10B. The SEM

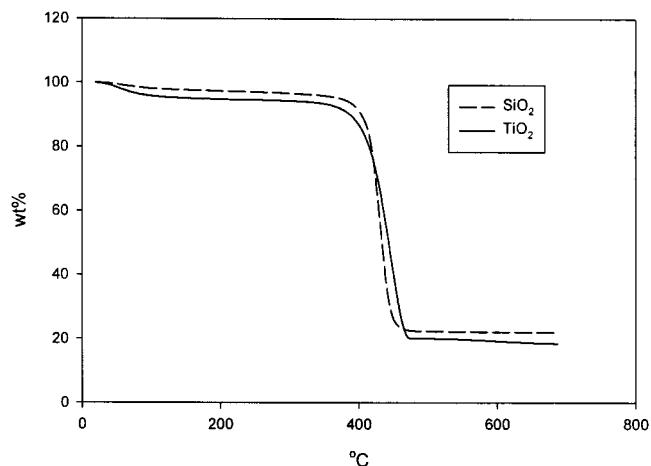


Figure 8. Thermal gravimetric analyses of titania–polystyrene (solid line) and silica–polystyrene (dashed line) composites. The samples were heated from 25 to 700 °C at 1.0 °C/min.

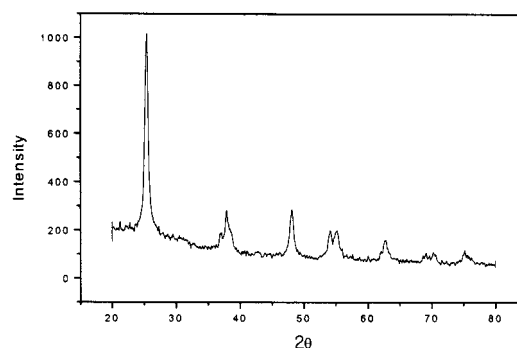


Figure 9. Powder X-ray diffraction pattern showing the presence of anatase in an ordered macroporous titania sphere.

image of Figure 10C indicates that the well-ordered macroporous structure is formed inside of the particle. The sites of the air cavities were occupied by the PS latex spheres. It can be noted that the air cavities (or cages) were interconnected and arranged into an fcc structure.

Ellipsoidal Shape. The suspension droplet can be deformed into either an oblate or a prolate spheroid depending on the electrical properties of the constituent phases. When the droplet phase is highly conducting compared to the continuous phase, the electric field deforms the drop into a prolate spheroid. Therefore, a highly conducting aqueous suspension droplet immersed in a less conducting oil phase deforms into an ellipsoid under the action of the electric field. Of course, the electric field strength should be lower than a certain critical value, above which the droplet cannot sustain its steady-state shape and eventually breaks up. In the present study, we prepared ellipsoidal particles by applying an ac electric field to the colloidal crystallization cell, as shown in Figure 2. The microscope image of Figure 11A shows the prepared ellipsoidal colloidal assembly of PS latex spheres. In this case, the strength of the ac electric field was 2.85 kV/cm at 60 Hz. Utilizing the ellipsoidal colloidal assemblies as templates, we prepared ellipsoidal macroporous titania particles from hydrolysis of the metal alkoxide (see the microscope image in Figure 11B). The SEM image of Figure 11C shows that the well-ordered macroporous structure is formed inside of the particle and the cavities are again

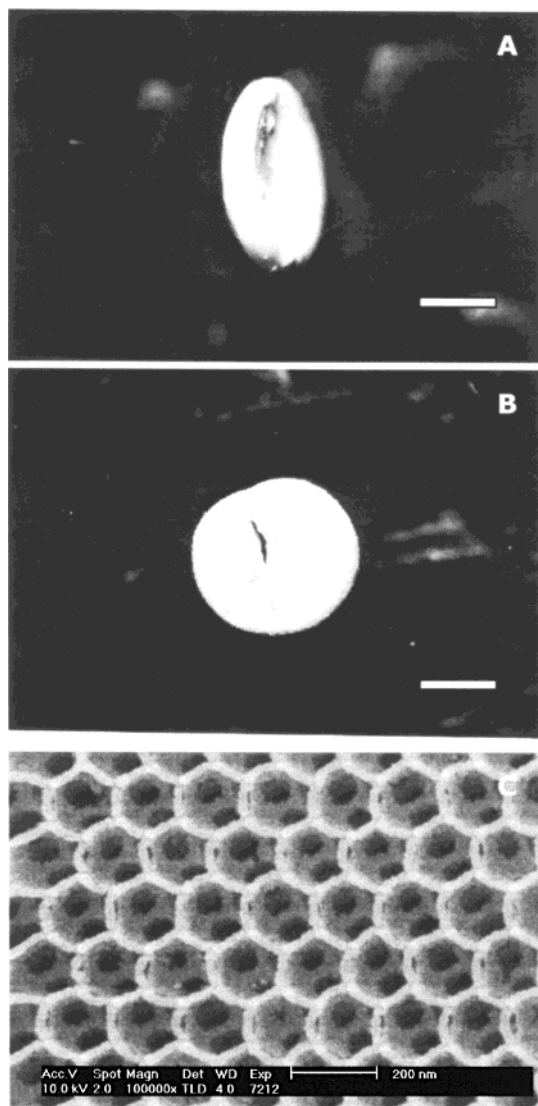


Figure 10. (A) Optical microscope image of a concave disklike colloidal assembly of PS latex spheres 230 nm in diameter. (B) Optical microscope image of a concave disklike macroporous titania particle that was prepared from the nonspherical colloidal assembly of the PS latex spheres. The scale bars in parts A and B denote 1 mm in length. (C) SEM image at large magnification showing the interconnected cavity pores.

interconnected. This clearly indicates that the electric field does not disturb the colloidal assembly of the PS latex spheres.

Summary

Ordered macroporous particles of titanium oxide and silicon oxide were fabricated by utilizing colloidal crystals as templates that were assembled through colloidal crystallization of aqueous suspension drops. The shape of the colloidal crystals was either spherical or nonspherical (oblate or prolate spheroids) and was successfully controlled by applying an ac electric field or by adding surfactant. The prepared macroporous materials showed three important morphological features. First, the macroporous particles were *regular* in macroscopic shape, such as spheres, ellipsoids, and concave disks with a length scale of a few millimeters. Second, the macroporous particles possessed very high internal surface areas, which were achieved via an *intercon-*

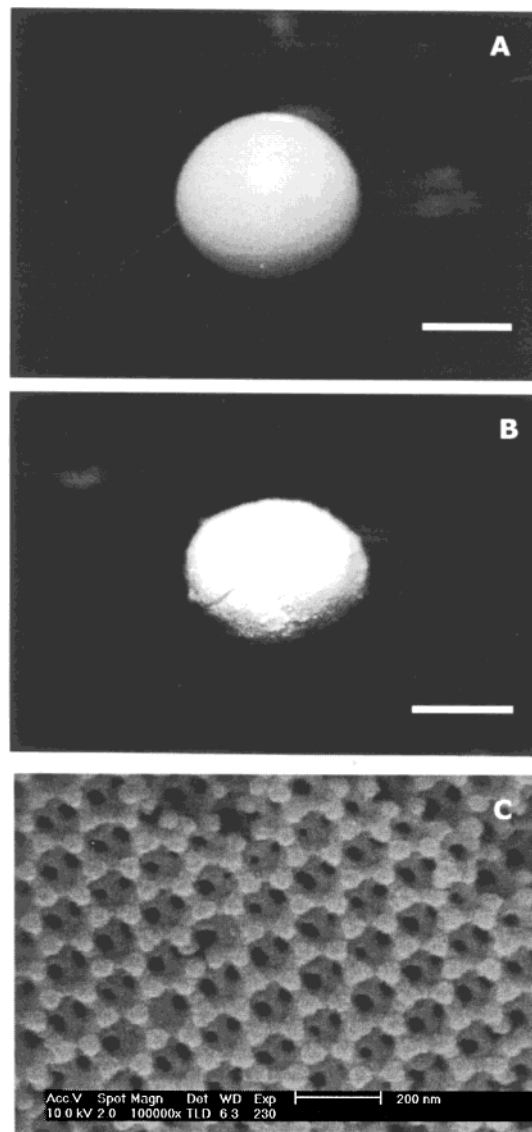


Figure 11. (A) Optical microscope image of an ellipsoidal colloidal assembly of PS latex spheres 190 nm in diameter. (B) Optical microscope image of a macroporous titania ellipsoid that was prepared from the nonspherical colloidal assembly of the PS latex spheres. The scale bars in parts A and B denote 1 mm in length. (C) SEM image at large magnification showing the interconnected cavity pores.

ected network of cavities a few hundred nanometers in diameter. These macrocrystalline ceramics with two distinctively different length scales have an extensive range of applications because of large porosity and chemical stability. Third, the interconnected cavities (or air bubbles) were ordered into the fcc lattice. The long-range ordering of the cavities endows the materials with striking optical properties that have received considerable attention in the past decade.

Acknowledgment. We would like to thank Kyeong Youl Jung for assistance with PXRD measurement, and Dr. Jeong-Jin Hong for many useful discussions. This work was supported by the Brain Korea 21 program. Jong Man Jung (Korea Basic Science Institute) is also acknowledged for his helpful guidance with the characterization of scanning electron microscopy data.